Journal of Engineering Science and Technology
Vol. 16, No. 3 (2021) 2394 - 2415

POWER QUALITY DISTURBANCES REPRESENTATION UTILISING SPECTROGRAM IN THE DISTRIBUTION SYSTEM

ALI B. MOHAMMED[1,*], AHMAD F. MOHAMAD[1], NORFAIZA F.[1], DANIAL M. NOR[1], SHIBLY A. AL-SAMARRAIE[2], B. MOHAMMED AL KADHIMI[3]

[1]Faculty of Electrical and Electronic Engineering, Universiti Tun Hussein Onn, 86400 Batu Pahat, Johor, Malaysia
[2]Department of Control and Systems Engineering, University of Technology, P.O. Box 18310, Al-Sina'a Street, 10066 Baghdad, Iraq
[3]Electrical Engineering Department, College of Engineering, Wasit University, Al-Kut, Wasit, Iraq
*Correspond author: alaoibasim2013@gmail.com

Abstract

Power quality significantly influences high-technology equipment applications in today's growing industry, especially for advanced control, communication, automation, on-line service, and precise manufacturing technique. Power quality problems like sag, swell, interruption, transients, and another distortion to the sinusoidal waveform, the dynamic voltage restore can be used to mitigate the disturbances at the distribution system. For instance, voltage sag can severely influence the products of semiconductor fabrication and cause financial losses. Almost all disturbances are represented in time-amplitude-based signal; the corrected signal has several harmonics which its frequency changes in time, which will result in difficulty in time-domain analysis. It is possible to propose time-frequency representation to the signal in this work to overcome these issues. The short-time Fourier transform (STFT) used in this paper to give a new representation of the signals when it is in the time-frequency domain. 2D will provide a better result for voltage disturbances than a normal voltage signal and makes it easier to calculate the signals' power spectral density.

Keywords: Dynamic voltage restorer (DVR), Short-time Fourier transform (STFT), Spectrogram, Voltage disturbance , Voltage sag.

1. Introduction

In recent years, power quality has received significant interest, in line with the concern over quality power distribution and transmission. Power quality could avoid common disturbances in the electric grid, such as voltage sag/ swell, flicker, and harmonics [1]. In the meantime, power quality problems can be defined as a deviation of current frequency and voltage from its standard values in the power system [2, 3]. The increased use of non-linear electronic control devices in electrical power systems could increase power quality deterioration. This means that more focus is needed by power industry agents [4]. However, from the perspective of industrial and commercial producers, the businesses and end-users are suffering in terms of money, time, and resources [2, 5]. In terms of power quality, voltage sag and swell are core problems in the power systems at the distribution and transmission sides. Voltage sag or voltage dip can be described as the short duration of voltage drop in RMS (root mean square) from its standard voltage value, which is lower than the nominal voltage range of 0.1 to 0.9 per unit (pu) between half-cycle to 1 minute. Based on the type of the fault, the voltage sags can either be unbalanced or balanced. However, they always have unpredictable scales. Voltage swell is characterized as the fast increment in RMS (root mean square) voltage value from the standard voltage over the ostensible esteem, extending from 1.1 to 1.8 (pu) for a half cycle to 1 minute. As a result, the vast burdens and stimulation of capacitor banks will be turned off, causing voltage swell [6]. The dynamic voltage restorer (DVR) utilized to mitigate the voltage disturbances such as voltage sag/swell and harmonics [7, 8]. The dynamic voltage restorer mounted between the grid and the sensitive loads via a series transformer [9, 10].

While there are considerable severe voltage disturbances, most of these disturbances are represented in time-amplitude based signal, since the corrected signal contains several harmonics which its frequency changes in time that will result in difficulty in time-domain analysis. It is possible to propose time-frequency representation to the signal in this work to overcome these issues, 2D will provide a better result for voltage disturbances than a normal voltage signal and makes it easier to calculate the signals' power spectral density. The technique has been extended into a 2D analysis by utilizing image processing techniques to obtain more information and a deeper understanding of when it is in the time-frequency domain of the voltage signal [11]. Once a 2D signal is obtained, the voltage raw signals need to be converted into Fourier Transform to analyse in frequency-based signals, which is in the time-based format. The voltage signals can be analysed in time-frequency-based signals known as a spectrogram [12]. There are various techniques for calculating the time-frequency density of signal energy like the short-time Fourier transform (STFT) [11] and Wigner Ville distributions (WVD) [11, 13]. Short-Time Fourier Transform is a popular method to analyse the time-frequency signal [11].

The Short-Time Fourier Transform (STFT) is widely used to convert signals from the time domain into a time-frequency representation. This representation has well-known limitations regarding time-frequency resolution. The STFT is implemented in the analysis of the power quality due to the ability to analyse the non-stationary signals, as is the case of the most powerful quality signals.

The STFT's key benefit is that it can provide the harmonic content of the signal in a pre-defined window during every time span. The frequency contents of the analysed power quality signals usually vary in only a short period of time, it is useful to use the time-frequency information [14]. The STFT is used to ascertain the frequency content of non-stationary signals at different time intervals is provided by Azam et al. [15]. The analysis of voltage disturbance signals in the time-frequency domain utilized STFT is given in [16]. STFT is utilized to analyse the terminal voltage of the induction machine to discover eccentricity-related faults as described in research by Nandi et al. [17]. Samantaray et al. [18], presented approach for protecting the transmission line utilizing STFT variable window on current and voltage signals. Power spectral density can describe as a mathematical quantity that determines the spectral of the signal content. Power spectral density describes how the signal power was distributed in frequency. CusidÓCusido et al. [19] describe a new approach to detecting the fault in motor is used by utilising a power spectral density and the wavelet techniques. The calculation of PSD to the pulse width modulation voltage source inverter (VSI) with randomized switching frequency is provided by Kirlin et al. [20].

2. Short Time Fourier Transform (STFT)

The output of from experiments commonly signal depends on time. Thus, the signal is represented in time-based. The scientist transforms a signal in time-based to a frequency-based utilising Fourier Transform (FT). Transforming signals into frequency-based is necessary because it ensures which signal is generated and extracts the frequency domain signals' important information. Usually, the signal is generated in a repeating pattern, which distinguishes the pure signal from noise. In practice, signals change over time, but in FT, the phase, amplitude and frequency do not change [21], requiring an algorithm that permits a signal change over time. Short-time Fourier Transform (STFT) is utilised to overcome this problem. Short-time Fourier Transform is defined in Eq. (1).

$$STFT\ (t,f) = \int_{-\infty}^{\infty} x(t)w(\tau - t)e^{-j2\pi ft}dt \quad (1)$$

where:

$x(t)$: Represents the distorted signals in time domain.

$w(t)$: Represents the window function used 1024.

STFT translates signal shifts that differ in time, just in a small segment (window) of the data at a time, by carrying out Fourier transform. It maps the signal into a two-dimensional frequency and time function. This is seen very clearly in Eq. 1, in which the signal STFT is the signal FT multiplied by the window function. However, in the signal processing that is called as a spectrogram, the squared value of short time Fourier transform is commonly utilised. The study of the spectrogram describes the three-dimensional imitation of the energy signal in relation to frequency and time as seen mathematically [22], in Eq. (2):

$$P\ (t,f) = \left|\int_{-\infty}^{\infty} x(t)w(\tau - t)e^{-j2\pi ft}dt\right|^2 \quad (2)$$

The Hanning window was selected because of its lower peak side loop, and it has a narrow influence on another frequency around the fundamental frequency value of 50 Hz [23]. In this study, windows size of 1024 used to do the analysis.

3. Power Spectral Density (PSD)

Power spectral density depicts the power of changes (energy) as a function of frequency. In another meaning, it indicates at which frequency variations are high and at which frequency variations are small. The PSD unit is energy per frequency and can produce energy within a given frequency range by integrating the PSD into that frequency range. PSD is a very helpful tool if you want to know the frequencies and amplitudes of oscillatory signals in time series results. The Fourier transforms expression of the time domain as shown as Eq. (3) below:

$$U\ (v) = \int_{-\infty}^{\infty} u(t) e^{-j2\pi vt} dt \tag{3}$$

Symbols v is the frequency variable, this expression utilises the positive convention in the Fourier kernel because this is popular in a scientific application. The transform has no additional scaling constant in its description. The area under $|U\ (v)|^2$ is the total energy in $u(t)$, can be written as Eq. (4):

$$\int_{-\infty}^{\infty} u^2(t) dt = \int_{-\infty}^{\infty} |U\ (v)|^2 dv \tag{4}$$

The energy spectral density can be defining as $E(v) = |U\ (v)|^2$ It has energy units per frequency unit. If the function $u(t)$ is not Fourier transformable but has a finite average power and can truncated as Eq. (5) below:

$$u_T(t) = \begin{cases} u(t) & \frac{T}{2} \leq t \leq \frac{T}{2} \\ 0 & otherwise \end{cases} \tag{5}$$

Which has the Fourier transform $\rho[u_T(t)] = U_T(v)$. If a function is Fourier transform, data sets are always discrete and truncated. $|U_T(v)|^2$ provides an energy distribution on the frequency for truncated signal $u_T(t)$, which can then be written as the normalized energy spectrum, Eq. (6):

$$G_T(v) = \frac{|U_T(v)|^2}{T} \tag{6}$$

It has power units per frequency unit. The PSD for $u_T(t)$ with width of T in signal space can give as Eq. (7) below [24]:

$$PSD(v) = G(v) = \lim_{T \to \infty} \frac{|U(v)|^2}{T} \tag{7}$$

4. The System Modelling and Simulation

The DVR-based system was investigated using MATLAB/Simulink to improve the disturbances in the distribution system like unbalanced or balanced voltage sag/swell, various forms of faults, and voltage imbalances. Dynamic voltage restorer applied with the distribution system is illustrated in Fig. 1. All information and data are obtained from Mohammed et al. [6], the disturbance cases are detailed below:

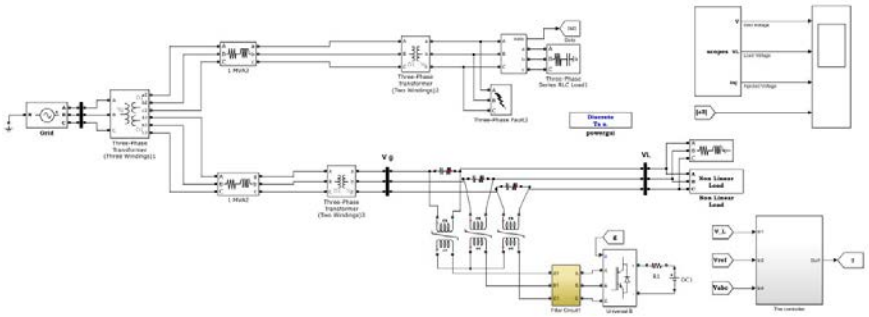

Fig. 1. System under study in MATLAB / Simulink.

5. Spectrogram Results

The results of the short-time Fourier transform (STFT) implementation are presented below.

5.1. Balance three-phase voltage sag

Balance voltage sag was applied to the system under study from 0.1 s to 0.15 s and induction motor from 0.185 s to 0.2 s. The resulting time-frequency representation is shown in Fig. 2(a)-(c).

The power spectral density of the signals for balanced voltage sag before and after the compensation is shown in Table 1.

As illustrated in Fig. 2(a)-(c) and Table 1, the lower power spectral density when the disturbance occurred in phase A, B, and C, is projected in Fig. 2. After compensation, the DVR injected a proper magnitude of the voltage with high power spectral density, represented in yellow.

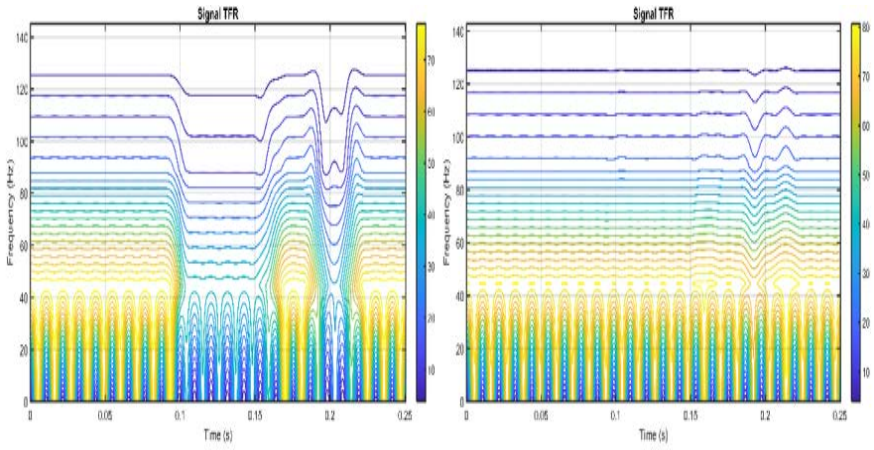

(a) Pre-and post-compensation phase A.

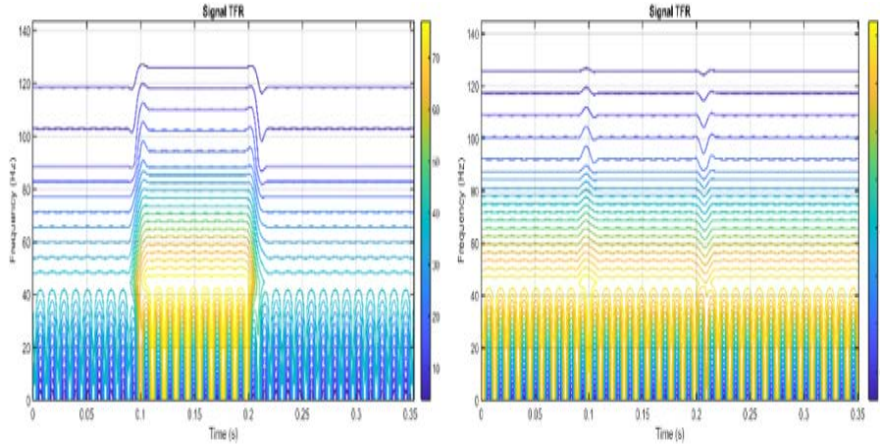

(b) Pre-and post-compensation phase B.

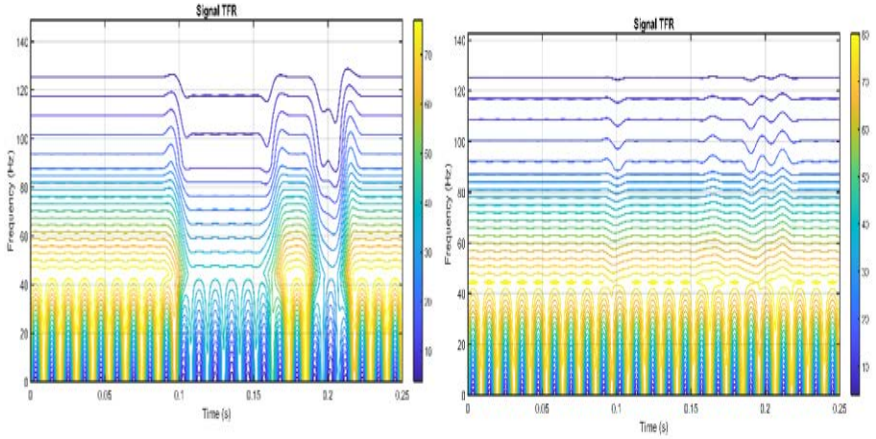

(c) Pre-and post-compensation phase C.

Fig. 2. Spectrogram results for the case of balance voltage sag.

Table 1. Power spectral density for balance voltage sag.

Case name	Power spectral density (W / Hz)					
	Before			After		
	A	B	C	A	B	C
Balance voltage sag	105.3906	105.1489	105.4870	128.1652	128.3239	128.1180

5.2. Deep balance voltage sag

The deep balanced voltage sag was implemented between 0.1 s to 0.2 s. The load voltage side decreased to 10%. The time-frequency representation is shown in Fig. 3 (a)-(c).

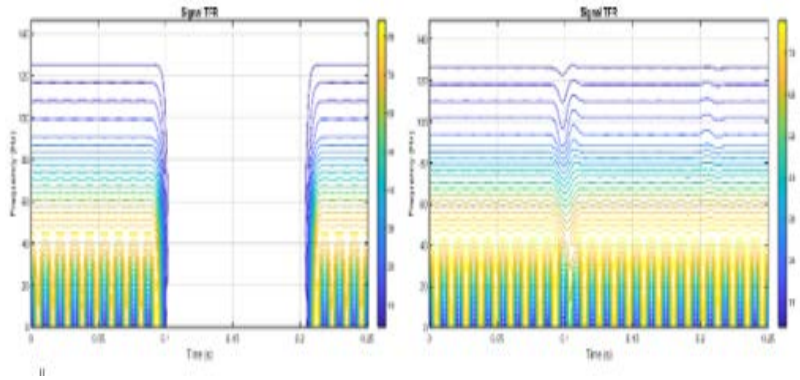

(a) Pre-and post-compensation phase A.

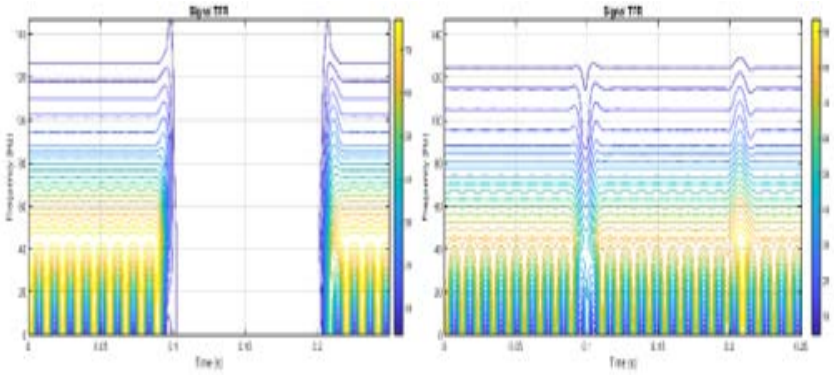

(b) Pre-and post-compensation phase B.

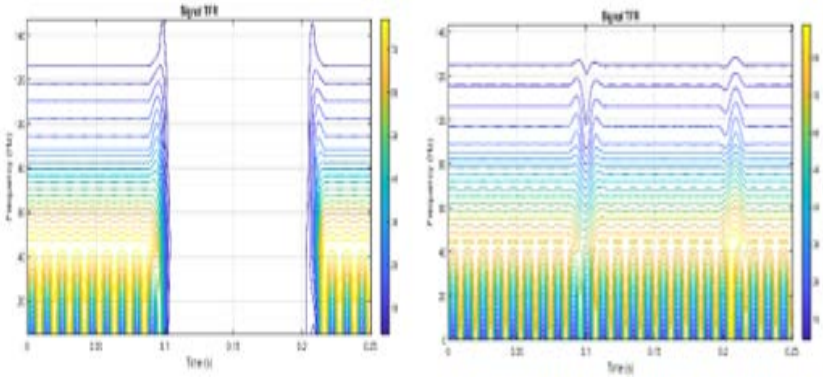

(c) Pre-and post-compensation phase C.

Fig. 3. Spectrogram results for the case of balance deep voltage sag.

The power spectral density of the signals for deep balanced voltage sag before and after the compensation is shown in Table 2.

There was a sudden halt where there is no power magnitude observed during the deep voltage sag occurrence. After compensation, the DVR regulated this halt

by injecting a proper voltage magnitude with high power spectral density represented in yellow.

Table 2. Power spectral density for deep balance voltage sag.

Case name	Power spectral density (W/Hz)					
	Before			After		
	A	B	C	A	B	C
Deep balance voltage sag	73.5377	72.6981	72.7	127.2479	127.5476	128.3471

5.3. Unbalanced voltage sag

The unbalanced voltage sag occurred at the interval time between 0.2 s - 0.3 s and the time duration of the disturbance is 0.1 s. The time-frequency representation is shown in Fig. 4(a)-(c).

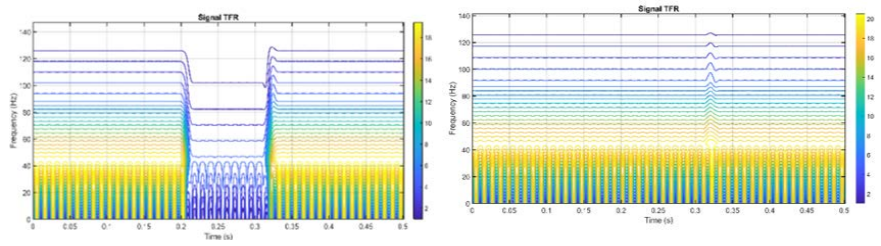

(a) Pre-and post-compensation phase A.

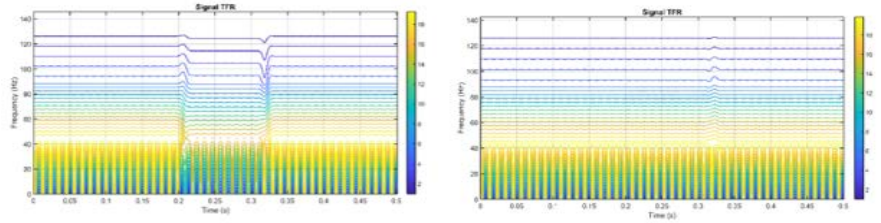

(b) Pre-and post-compensation phase B.

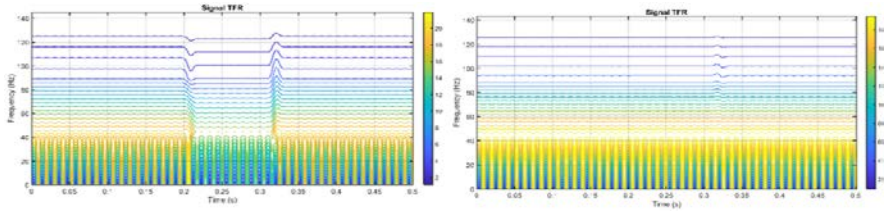

(c) Pre-and post-compensation phase C.

Fig. 4. The spectrogram results for the case of unbalanced voltage sag.

The power spectral density of the signals for the unbalanced voltage sag before and after the compensation is shown in Table 3.

Table 3. Power spectral density for unbalanced voltage sag.

Case name	Power spectral density (W / Hz)					
	Before			After		
	A	B	C	A	B	C
Unbalance voltage sag	28.0888	31.9835	32.1570	33.5612	33.5125	33.5096

As illustrated in Fig. 4(a)-(c) and Table 3, when the unbalanced voltage sag occurred in Phase A, B and C, there is a lower power spectral density as projected in blue. In this light, the different magnitudes of power depend on the disturbance's depth at that Phase. After compensation, the DVR injected a proper magnitude of voltage with a high magnitude of power spectral density as represented in yellow.

5.4. Balanced three-phase voltage swell

The balance voltage swell applied to the system. The voltage swell occurred between t = 0.1 s and t = 0.2 s. The time-frequency representation is shown in Fig. 5(a)-(c).

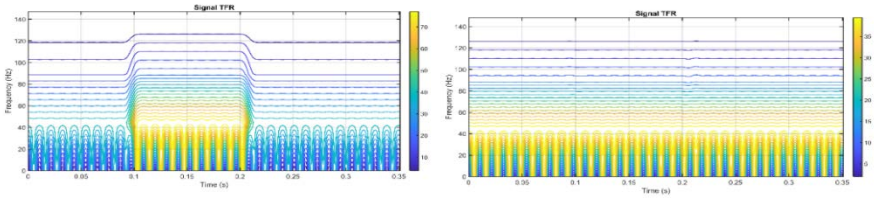

(a) Pre-and post-compensation phase A.

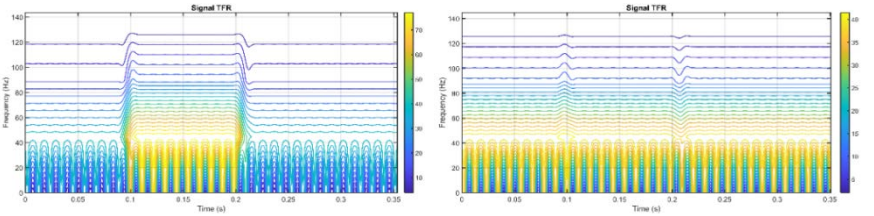

(b) Pre-and post-compensation phase B.

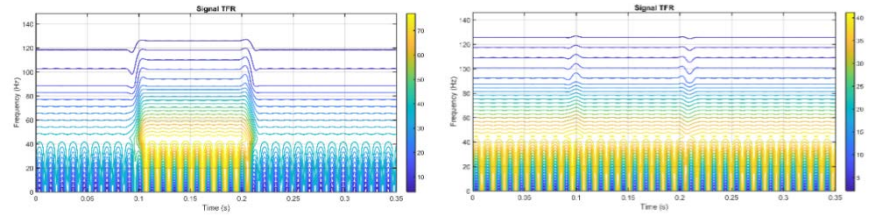

(c) Pre-and post-compensation phase C.

Fig. 5. The spectrogram results for the case of balance voltage swell.

The power spectral density of the signals for balance voltage-swell before and after the compensation is shown in Table 4.

Table 4. Power spectral density for balance voltage swells.

Case name	Power spectral density (W / Hz)					
	Before			After		
	A	B	C	A	B	C
Balance voltage swell	86.5273	86.4373	86.4372	67.1328	67.0941	67.1064

When the balanced voltage swell occurred in the distribution system, phase A, B, and C show a high-power spectral density as represented by the yellow colour at the time of the disturbance. After compensation, the DVR regulated the power by injecting a proper magnitude of voltage. As a result, the yellow colour was spread equally across the timeline.

5.5. Deep balanced voltage swell

In this case, the deep swell mode occurred from 0.1 to 0.2 s which increased the voltages at the load side to 180%. The time-frequency representation is shown in Fig. 6(a)-(c).

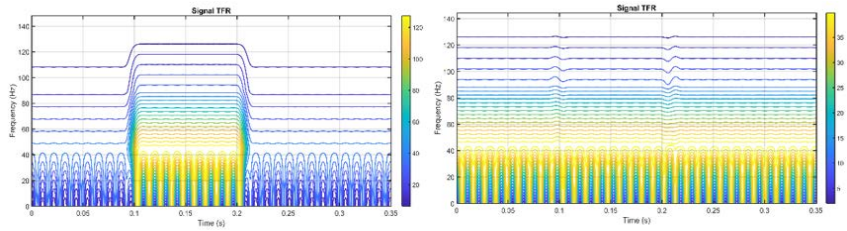

(a) Pre-and post-compensation phase A.

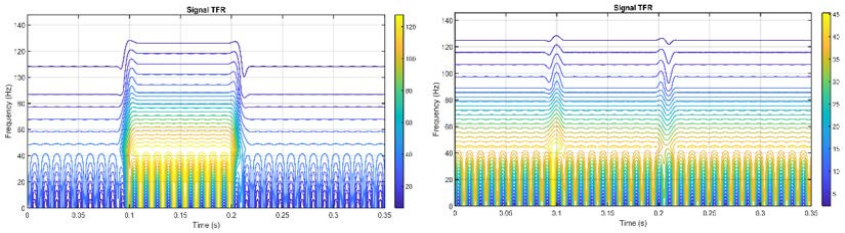

(b) Pre-and post-compensation phase B.

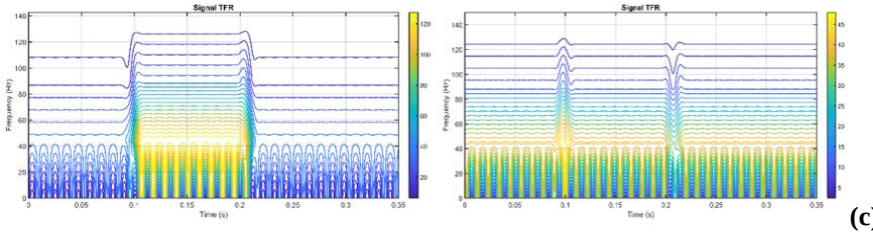

(c) Pre-and post-compensation phase C.

Fig. 6. The spectrogram results for the case of deep balance voltage swell.

The power spectral density of the signals for deep balance voltage- swell before and after the compensation is shown in Table 5.

Table 5. Power spectral density for deep balance voltage swell.

Case name	Power spectral density (W / Hz)					
	Before			After		
	A	B	C	A	B	C
Deep balance voltage swell	112.7261	112.4766	112.4769	67.1248	67.2514	67.2407

When the deep balance voltage swell occurred, phase A, B and C have a very high-power spectral density as reflected by the yellow colour at the time of the disturbance. After compensation, the DVR regulated the power by injecting a proper magnitude of voltage to make the yellow colour spreads almost equally across the timeline.

5.6. Unbalance voltage swell

This type involved unbalanced voltage swell which occurred from 0.2 s to 0.3 s. The duration of this disturbance is 0.1 s. The time-frequency representation is shown in Fig. 7(a)-(c).

The power spectral density of the signals for unbalanced voltage-swell before and after the compensation is shown in Table 6.

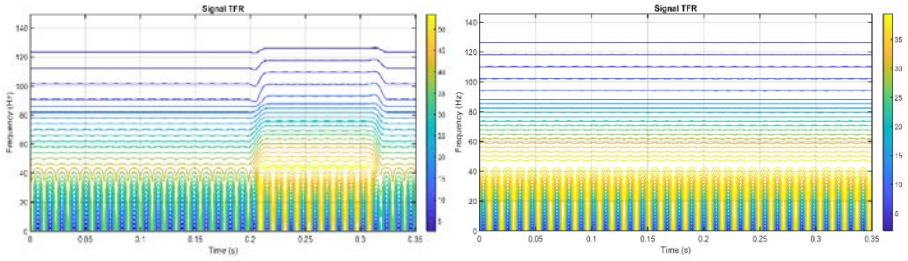

(a) Pre-and post-compensation phase A.

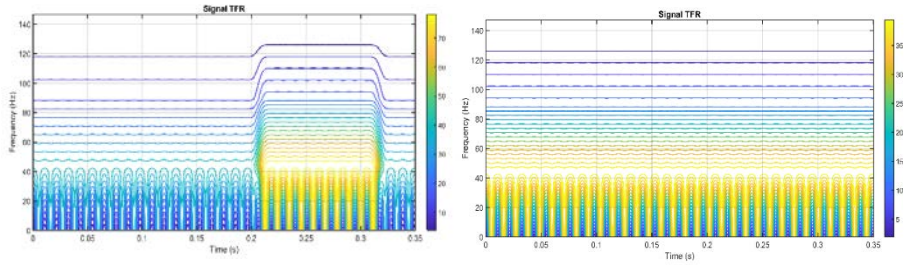

(b) Pre-and post-compensation phase B.

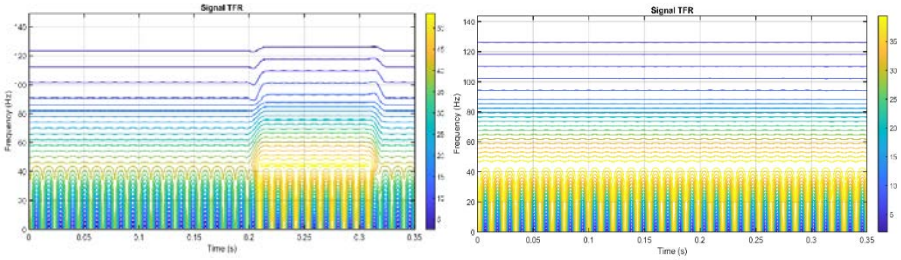

(c) Pre-and post-compensation phase C.

Fig. 7. The spectrogram results for the case of unbalanced voltage swell.

Table 6. Power spectral density for unbalanced voltage swells.

Case name	Power spectral density (W / Hz)					
	Before			After		
	A	B	C	A	B	C
Unbalance voltage swell	87.1032	73.3951	72.3695	67.1339	67.1120	67.0766

When the unbalanced voltage swell occurred, phase A, B, and C show a high-power spectral density which appears in yellow in Fig. 7. In this light, the magnitude of the power depends on the disturbance's depth at that phase. After compensation, the DVR regulated the power by injecting a proper voltage magnitude to make the yellow colour spread almost equally across the timeline.

5.7. Three-phase short circuit (LLL-G)

The system under study was faced to a three-phase short circuit at 0.05 s. This fault occurred at Feeder one for 0.13 s. The time-frequency representation is shown in Fig. 8(a)-(c).

The power spectral density of the signals for the three-phase short circuit before and after the compensation is shown in Table 7.

As illustrated in Fig. 8. and Table 7, when the disturbance occurred, phase A, B, and C have a lower power spectral density which appears in blue. After compensation, the DVR injected a proper magnitude of voltage with a high magnitude of power spectral density represented by the yellow colour.

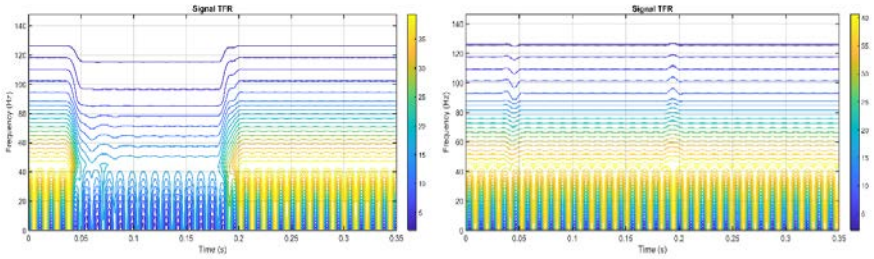

(a) Pre-and post-compensation phase A.

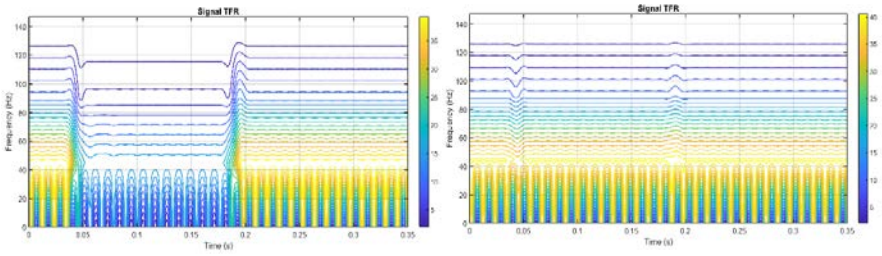

(b) Pre-and post-compensation phase B.

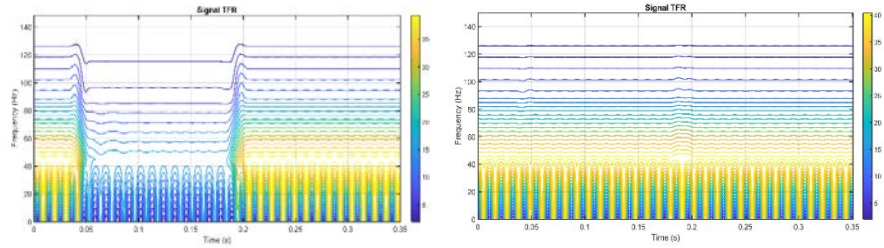

(c) Pre-and post-compensation phase C.

Fig. 8. Spectrogram results for the case of three phase short circuit.

Table 7. Power spectral density for three-phase short circuit.

Case name	Power spectral density (W / Hz)					
	Before			After		
	A	B	C	A	B	C
Three phase short circuit	51.2908	51.1982	51.0580	67.2254	67.0500	67.0997

5.8. Double line to ground fault (LL-G)

It was observed that Phase A and B suffer from double line to ground fault at 0.1 s. The duration of the fault was added for 0.1 s. The time-frequency representation is shown in Fig. 9(a)-(c).

The power spectral density of the signals for the double line to a ground fault before and after the compensation is shown in Table 8.

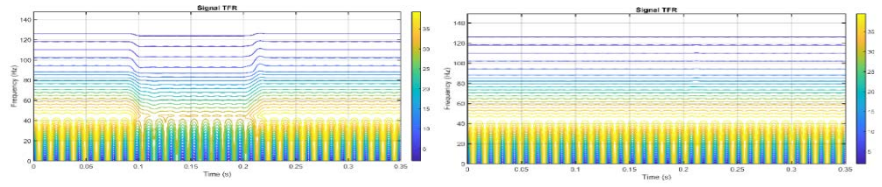

(a) Pre-and post-compensation phase A.

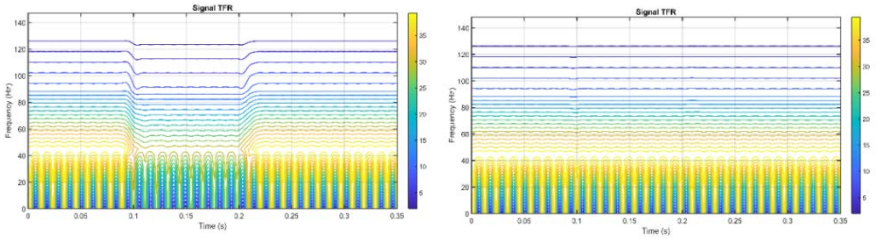

(b) Pre-and post-compensation phase B.

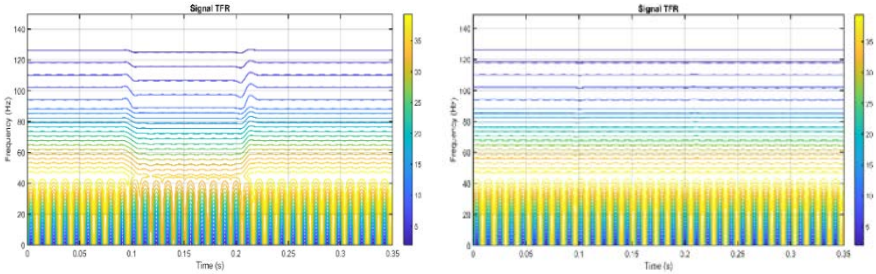

(c) Pre-and post-compensation phase C.

Fig. 9. Spectrogram results of the case of the double line to ground fault.

Table 8. Power spectral density for double line to ground fault.

Case name	Power spectral density (W / Hz)					
	Before			After		
	A	B	C	A	B	C
Double line to ground fault	62.1748	61.6443	64.3335	66.9827	66.9190	66.9270

As illustrated in Fig. 9. and Table 8, when the disturbance occurred, Phase A, B, and C have a lower power spectral density reflected by the blue colour. After compensation, the DVR injected a proper magnitude of voltage with a high magnitude of power spectral density, represented in yellow.

5.9. Single line to ground fault (L-G)

This case is significant for the analysis as the most frequent fault in operation is the single line to ground fault, which occurred at Phase C. This fault started at 0.05 s and stopped at 0.185 s. Compared to the above situations, the fault occurred at Feeder 1. The time-frequency representation is shown in Fig. 10(a)-(c).

The power spectral density of the signals for a single line to a ground fault before and after the compensation is shown in Table 9.

As illustrated in Fig. 10. and Table 9, when the disturbance occurred, phase A, B, and C have a lower power spectral density reflected by the blue colour. The DVR injected a proper magnitude of the voltage with a high magnitude of the power spectral density as represented in yellow.

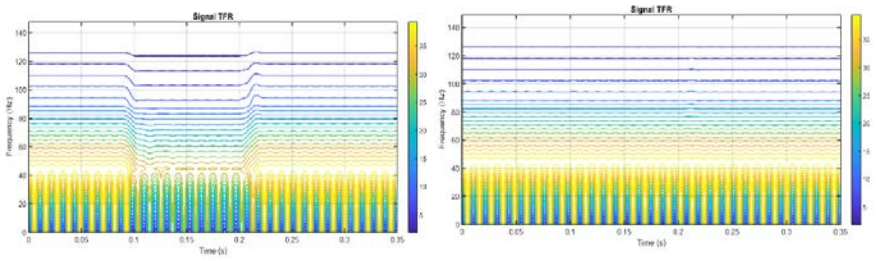

(a) Pre-and post-compensation phase A.

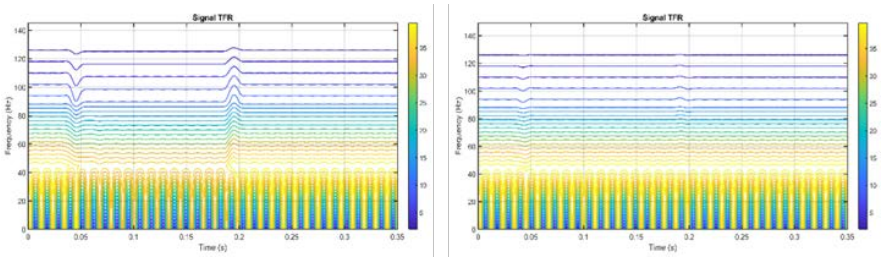

(b) Pre-and post-compensation phase B.

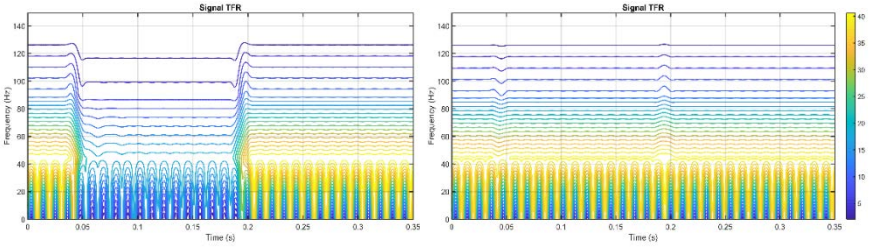

(c) Pre-and post-compensation phase C.

Fig. 10. The spectrogram results for the case of a single line to ground fault.

Table 9. Power spectral density for single line to ground fault.

Case name	Power spectral density (W / Hz)					
	Before			After		
	A	B	C	A	B	C
Single line to ground fault	62.0868	64.2758	51.9124	67.1310	67.0678	67.0975

5.10. Voltage imbalance

In this scenario, the system was exposed to an imbalanced voltage between 0.05 s and 0.185 s. The duration of disturbance is equal to 0.135 s. The time-frequency representation is shown in Fig. 11(a)-(c).

The power spectral density of the signals for voltage imbalance before and after the compensation is shown in Table 10.

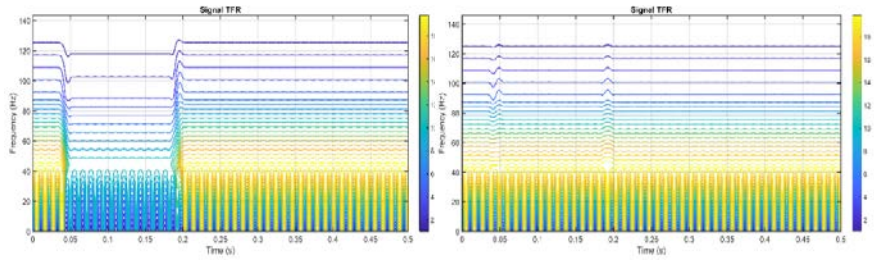

(a) Pre-and post-compensation phase A.

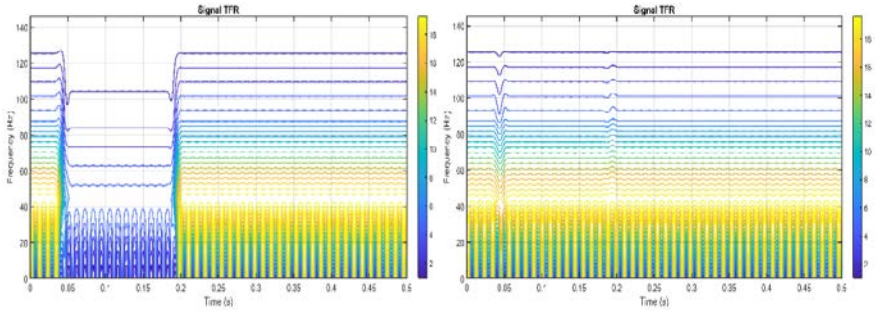

(b) Pre-and post-compensation phase B.

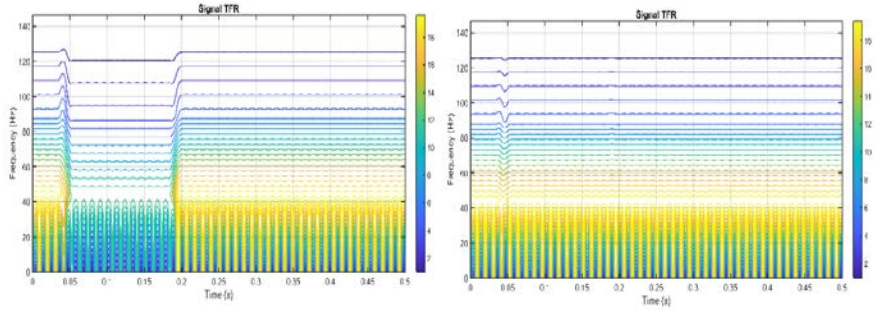

(c) pre-and post-compensation phase C.

Fig. 11. The spectrogram results for the case of voltage imbalance.

Table 10. Power spectral density for voltage imbalance.

Case name	Power spectral density (W / Hz)					
	Before			After		
	A	B	C	A	B	C
Voltage imbalance	28.9520	26.4310	29.9811	33.5444	33.4240	33.4630

As illustrated in Fig. 11. and Table 10, when the imbalance voltage occurred, Phase A, B, and C have a lower power spectral density, which is reflected by the blue colour. In this regard, the magnitude of the power depends on the disturbance's depth at that phase. At compensation, the DVR injected a proper magnitude of voltage with a high magnitude of power spectral density as represented in yellow.

5.11. Transients

A power quality index appeared as the amplitude of voltage became very high. At the same time, there was a decrease in non-power frequency for a very brief span. It can be separated into two, latent oscillating and impulsive. The temporary impulsive transients are integrated as lightning strikes when the voltage magnitude rapidly increased or decreased for a very brief period, specifically lower than 50 ns. The time-frequency representation is illustrated in Fig. 12(a)-(c).

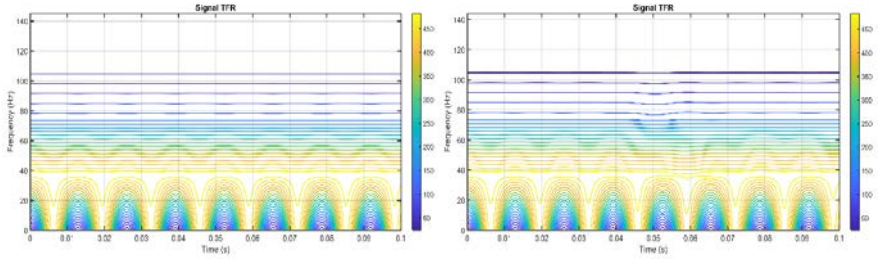

(a) Pre-and post-compensation phase A.

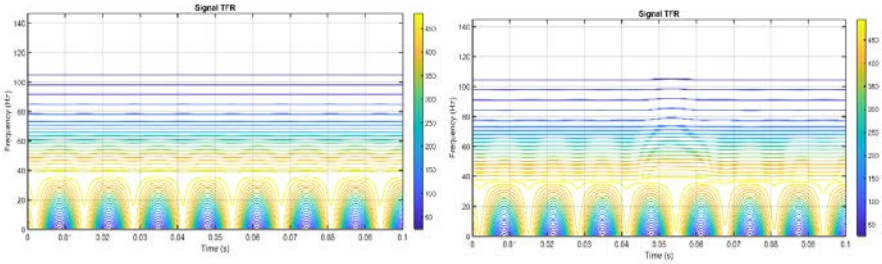

(b) Pre-and post-compensation phase B.

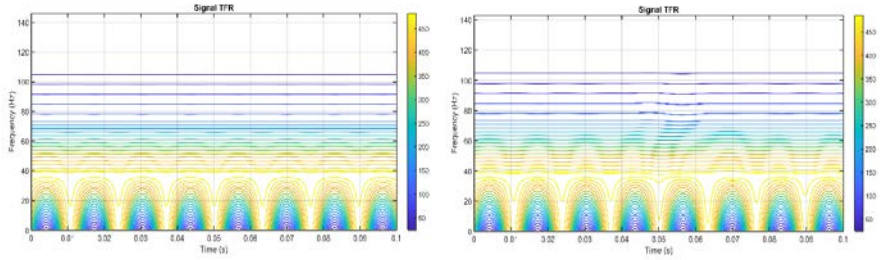

(c) Pre-and post-compensation phase C.

Fig. 12. The spectrogram results for the case of impulsive transient.

The power spectral density of the signals for impulsive transient before and after the compensation is shown in Table 11.

As illustrated in Fig. 12. and Table 11, when the impulsive transient occurred, Phase A, B, and C have a lower power spectral density reflected in the blue colour. In this regard, the magnitude of the power depends on the disturbance's depth at that Phase. At compensation, the DVR injected a proper magnitude of the voltage with a high magnitude of power spectral density as represented in yellow. The

second case that demonstrates the oscillatory voltage transient is the high-voltage capacitor bank created in Simulink. The time-frequency representation is shown in Fig. 13(a)-(c).

Table 11. Power spectral density for impulsive transient.

Case name	Power spectral density (W/Hz)					
	Before			After		
	A	B	C	A	B	C
Impulsive transient	694.9900	693.3934	693.3782	693.2359	697.1561	693.5332

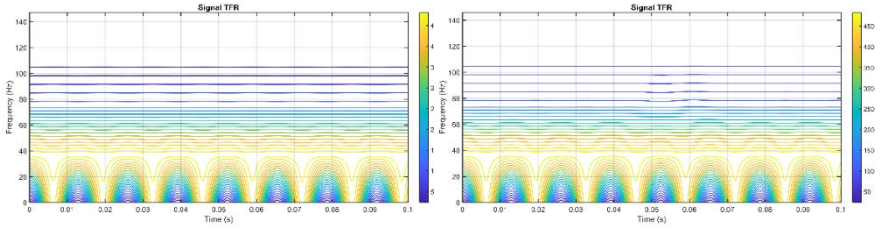

(a) Pre-and post-compensation phase A.

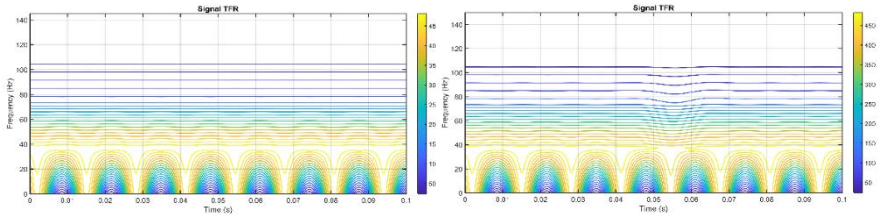

(b) Pre-and post-compensation phase B.

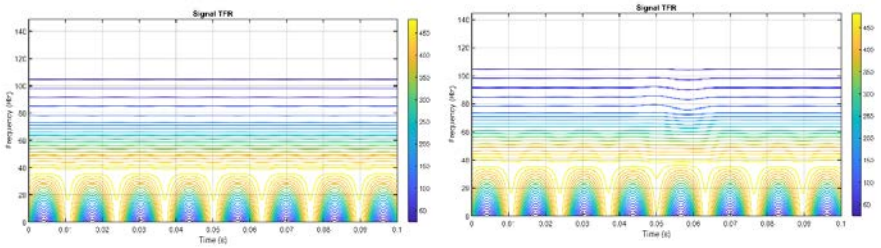

(c) Pre-and post-compensation phase C.

Fig. 13. Spectrogram results of the case of oscillatory voltage transient.

The power spectral density of the signals for oscillatory transient before and after the compensation is shown in Table 12.

As illustrated in Fig. 13 and Table 12, when the oscillatory transient occurred phase A, B, and C have a lower power spectral density as reflected in the blue colour. The magnitude of the power depends on the depth of the disturbance at that

Phase. After compensation, the DVR injected a proper magnitude of the voltage with a high magnitude of power spectral density represented in yellow.

Table 12. Power spectral density for oscillatory transient.

Case name	Power spectral density (W/Hz)					
	Before			After		
	A	B	C	A	B	C
Oscillatory transient	693.7215	697.5792	696.4283	695.2480	694.5579	695.8249

5.12. Voltage notching

Voltage notching is a normal transient induced by the electronic converter commutation process. The non-linear load model used a six-pulse three-phase rectifier to pose voltage notches and harmonics. The time-frequency representation is shown in Fig. 14(a)-(c).

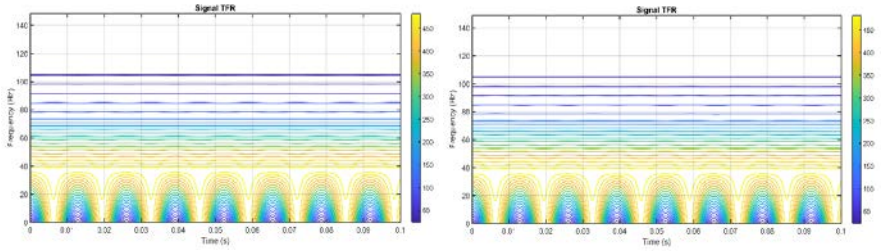

(a) Pre-and post-compensation phase A.

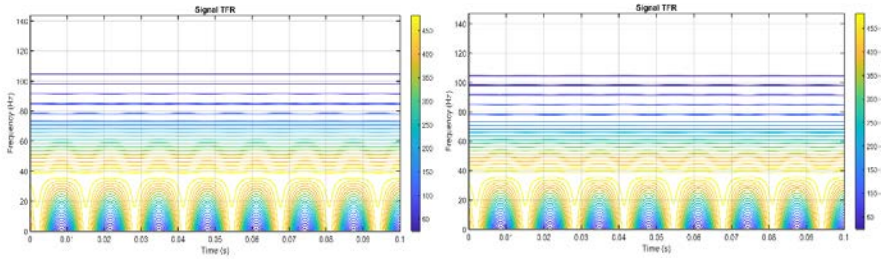

(b) Pre-and post-compensation phase B.

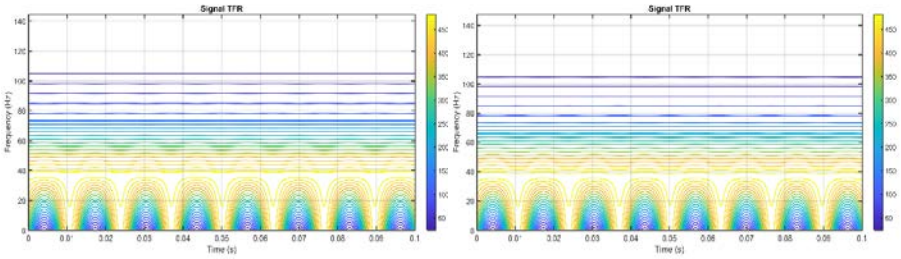

(c) Pre-and post-compensation phase C.

Fig. 14. Spectrogram results for the case of notching.

The power spectral density of the signals for notching before and after the compensation is shown in Table 13.

Table 13. Power spectral density for notching.

Case name	Power spectral density (W/Hz)					
	Before			After		
	A	B	C	A	B	C
Voltage notching	694.7281	693.1445	693.1237	693.6011	692.0511	692.2042

As illustrated in Fig. 14. and Table 13, at the voltage notching occurred, phase A, B, and C have a lower power spectral density as reflected in the blue colour. The different magnitude of the power depends on the depth of the disturbance at that Phase. After compensation, the DVR injected a proper magnitude of the voltage with a high magnitude of power spectral density as represented in yellow.

6. Conclusion

In this research, a 2D Voltage Disturbance (VD) data has been successfully produced using the image processing technique (spectrogram) and Short Time Fourier Transform (STFT) technique as well as calculating the power spectral density (PSD) of the signals.

There are considerable severe voltage disturbances, most of these disturbances are represented in time-amplitude based signal, Since the corrected signal contains several harmonics which its frequency changes in time, that will result to the difficulty in time domain analysis. It is possible to propose time-frequency representation to the signal in this work to overcome these issues.

2D will provide a better result for voltage disturbances than a normal voltage signal. The results have shown that the STFT activities and provide more details on the signals when a time-frequency presentation is presented. Simultaneously, the power spectral density results for all cases provide a detailed description of the accuracy of the proposed DVR controller in returning the signals to their original level before the faults occur.

References

1. Rauf, A.M.; and Khadkikar, V. (2014). An enhanced voltage sag compensation scheme for dynamic voltage restorer. *IEEE Transactions on Industrial Electronics*, 62(5), 2683-2692.
2. Francis, D.; and Thomas, T. (2014). Mitigation of voltage sag and swell using dynamic voltage restorer. Proceedings of *2014 Annual International Conference on Emerging Research Areas: Magnetics, Machines and Drives*, Kottayam, India,, 1-6.
3. Moghassemi, A.; and Padmanaban, S. (2020). Dynamic voltage restorer (DVR): A comprehensive review of topologies, power converters, control methods, and modified configurations. *Energies*, *13*(16).
4. Alam, M.R.; Muttaqi, K.M.; and Bouzerdoum, A. (2014). Characterizing voltage sags and swells using three-phase voltage ellipse parameters.

Proceeding of 2014 IEEE Industry Application Society Annual Meeting, Vancouver, Canada, 1-9

5. Al Kadhimi, B.M.; and Basim, A. (2020). Reduction of energy losses within electrical industrial system. *Journal of Green Engineering*, 10(9), 4851-4873.
6. Mohammed, A.B.; Ahmad f.M.N.; Norfaiza F.; Danial M.N.; and Shibly A.A. S. (2020). The improvement of controller based on dynamic voltage restorer (DVR) for distribution system. *Journal of Green Engineering*, 10, 7222-7277.
7. Mohammed, A.B.; Ariff, M.A.M.; and Ramli, S.N. (2020). An improved method for efficient controlling of the dynamic voltage restorer to enhance the power quality in the distribution system. *International Journal of Power Electronics and Drive System*, 11(4), 1958-1965.
8. Al-Kadhimi, B.M.; and Mohammed, A.B. (2020). The aspect of power quality in a wind generation: Overview. *Journal of Physics: Conference Series*, 1530(1).
9. Mohammed, A.B.; Ariff, M.A.M.; and Ramli, S.N. (2020). Power quality improvement using dynamic voltage restorer in electrical distribution system: An overview. *Indonesian Journal of Electrical Engineering and Computer Science*, 17(1), 86-93.
10. Mohammed, A.B.; and Ariff, M.A.M. (2020). The enhancement of power quality for the distribution system via dynamic voltage restorer. *International Journal of Power Electronics and Drive Systems*, 11(3), 1588-1595.
11. Saad, M.H.M.; Nor, M.J.M.; Bustami, F.R.A.; and Ngadiran, R. (2007). Classification of heart abnormalities using artificial neural network. *Journal of Applied Sciences*, *7*(6), 820-825.
12. Mustafa, M.; Taib, M.N.; Murat, Z.; Sulaiman, N.; and Aris, S.A.M. (2011, March). The analysis of EEG spectrogram image for brainwave balancing application using ANN. *Proceedings of 2011 UkSim 13th International Conference on Computer Modelling and Simulation*, Cambridge, UK, 64-68.
13. Papandreou-Suppappola, A.; and Suppappola, S.B. (2002). Analysis and classification of time-varying signals with multiple time-frequency structures. *IEEE Signal Processing Letters*, 9(3), 92-95.
14. Gargoom, A.M. (2007). *Digital Signal Processing Techniques for Improving the Automatic Classification of Power Quality Events*, PhD Thesis, University of Adelaide.
15. Azam, M.S.; Tu, F.; Pattipati, K.R.; and Karanam, R. (2004). A dependency model-based approach for identifying and evaluating power quality problems. *IEEE Transactions on Power Delivery*, 19(3), 1154-1166.
16. Gu, Y.H.; and Bollen, M.H. (2000). Time-frequency and time-scale domain analysis of voltage disturbances. *IEEE Transactions on Power Delivery*, 15(4), 1279-1284.
17. Nandi, S.; Ilamparithi, T.C.; Lee, S.B.; and Hyun, D. (2010). Detection of eccentricity faults in induction machines based on nameplate parameters. *IEEE Transactions on Industrial Electronics*, 58(5), 1673-1683.
18. Samantaray, S.R.; and Dash, P.K. (2008). Transmission line distance relaying using a variable window short-time Fourier transform. *Electric Power Systems Research*, 78(4), 595-604.

19. CusidÓCusido, J.; Romeral, L.; Ortega, J.A.; Rosero, J. A.; and Espinosa, A. G. (2008). Fault detection in induction machines using power spectral density in wavelet decomposition. *IEEE Transactions on Industrial Electronics*, *55*(2), 633-643.
20. Kirlin, R.L.; Bech, M.M.; and Trzynadlowski, A.M. (2002). Analysis of power and power spectral density in PWM inverters with randomized switching frequency. *IEEE Transactions on Industrial Electronics*, 49(2) 486-499.
21. Fu, K.S.; and Rosenfield. (1976). Pattern recognition and image processing. *IEEE Transactions on Computers*, C-25(12), 1336-1346.
22. Tee, W.; Yusoff, M.R.; Abdullah, A.R.; Jopri, M.H.; Anwar, N.S.N.; and Musa, H. (2019). Spectrogram based window selection for the detection of voltage variation. *International Journal of Integrated Engineering*, 11(3).
23. Jopri, M.H.; Abdullah, A.R.; Manap, M.; Yusoff, M.R.; Sutikno, T.; and Habban, M.F. (2017). An improved detection and classification technique of harmonic signals in power distribution by utilizing spectrogram. *International Journal of Electrical and Computer Engineering*, 7(1), 12.
24. Youngworth, R.N.; Gallagher, B.B.; and Stamper, B.L. (2005). An overview of power spectral density (PSD) calculations. *Optical Manufacturing and Testing VI*,5869.